

A microscopic mechanism for increasing thermoelectric efficiency

Keiji Saito^{a,b}, Giuliano Benenti^{c,d}, Giulio Casati^{c,d,e}

^a*Department of Physics, Graduate School of Science, University of Tokyo, Tokyo 113-0033, Japan*

^b*Department of Physics, Graduate School of Science, 2 CREST, JST, 4-1-8 Honcho Kawaguchi, Saitama, 332-0012, Japan*

^c*CNISM, CNR-INFM, and Center for Nonlinear and Complex Systems, Università degli Studi dell'Insubria, Via Valleggio 11, 22100 Como, Italy*

^d*Istituto Nazionale di Fisica Nucleare, Sezione di Milano, Via Celoria 16, 20133 Milano, Italy*

^e*Centre for Quantum Technologies, National University of Singapore, Singapore 117543*

Abstract

We study the coupled particle and energy transport in a prototype model of interacting one-dimensional system: the disordered hard-point gas, for which numerical data suggest that the thermoelectric figure of merit ZT diverges with the system size. This result is explained in terms of a microscopic mechanism, namely the local equilibrium is characterized by the emergence of a broad stationary “modified Maxwell-Boltzmann velocity distribution”, of width much larger than the mean velocity of the particle flow.

Keywords: Thermoelectricity, Nonlinear dynamics, Onsager coefficients

PACS: 05.60.Cd, 84.60.Rb, 05.45.Pq

1. Introduction

Thermoelectricity is an old field: The Seebeck effect, that is, the conversion of temperature differences into electricity, was discovered in 1821. However, a strong interest in termoelectric phenomena arose only in the 1950's, when Ioffe discovered that doped semiconductors exhibited much larger thermoelectric effect than did other materials. He also proposed that semiconductors could be used to build solid-state home refrigerators. Such refrigerators would be long-lived, silent, maintenace-free, and environmentally

benign. Ioffe's suggestion initiated an intense research activity in semiconductors physics [1, 2, 3]. However, in spite of all efforts and consideration of all type of semiconductors, thermoelectric refrigerators have still poor efficiencies compared to compressor-based refrigerators. Today, thermoelectric devices are mainly used in situations in which reliability and quiet operation are more important than the cost. Applications include equipments in medical applications, space probes, etc.

In the last decade there has been an increasing pressure to find better thermoelectric materials with higher efficiency. The reason is the strong environmental concern about chlorofluorocarbons used in most compressor-based refrigerators. Also the possibility to generate electric power from waste heat using thermoelectric effect is becoming more and more interesting [1, 2, 3, 4].

The thermodynamic efficiency can be conveniently written in terms of the so-called figure of merit $ZT = (\sigma S^2/\kappa)T$, where σ is the electric conductivity, S the thermoelectric power (Seebeck coefficient), κ the thermal conductivity, and T the temperature. Ideal Carnot efficiency is recovered in the limit $ZT \rightarrow \infty$. In spite of the worldwide research efforts for identifying thermoelectric materials with high ZT values, so far the best thermoelectric materials are characterized by values of $ZT \sim 1$, at room temperature. Values $ZT > 3$ are considered to be essential for thermoelectric devices to compete in efficiency with mechanical power generation and refrigeration.

The challenge lies in engineering a material for which the values of σ , S , and κ can be controlled in order to optimize thermoelectric efficiency. The problem is that the different transport coefficients are interdependent, thus making optimization extremely difficult. On the other hand, thermodynamics does not impose any upper bound on ZT , so that efficient thermoelectric devices could in principle be engineered. The present understanding of the possible microscopic mechanisms leading to an increase of ZT is quite limited, with few exceptions. Notably, Refs. [5, 6] showed that the optimal density of states in a thermoelectric material is a delta function. Such sharp energy filtering allows to reach, in principle, the Carnot efficiency.

Here we consider the problem of increasing thermoelectric efficiency from a new perspective, that is, we pursue a dynamical system approach. Understanding from first principles and from nonlinear dynamics simulations the microscopic mechanisms that can be implemented to control the heat flow [7] might prove useful not only for thermoelectric phenomena but also for the design and engineering of thermal diodes and transistors. In this paper, our

plan is to compute transport coefficients and thermoelectric efficiency from first principles, namely from the underlying microscopic dynamical processes which are known to be predominantly nonlinear in nature. In a previous work [8], the thermoelectric problem has been investigated by numerical solution of the microscopic equations of motion. Inspired by the kinetic theory of ergodic gases and chaotic billiards, a simple microscopic mechanism for increasing thermoelectric efficiency was proposed. More precisely, the cross transport of particles and energy in open classical ergodic billiards was considered. It has been shown that, in the linear response regime, the thermoelectric efficiency can approach Carnot efficiency for sufficiently complex charge carrier molecules. Indeed, the figure of merit has been found to be a growing function of the number d_{int} of internal degrees of freedom, $ZT = (d + 1 + d_{\text{int}})/2$, where d is the geometric dimension.

In spite of the abstract nature of the model, the above paper opens the possibility for a theoretical understanding of the basic microscopic requirements that a classical dynamical system must fulfill in order to lead to a high thermoelectric figure of merit. In particular, the question arises whether inter-particle interaction might increase the effective number of degrees of freedom, thus leading to a higher figure of merit than in the noninteracting idealized d dimensional gas, where $ZT = (d + 1)/2$. Along these lines a detailed numerical study of the cross heat and particle transport has been performed for an open one-dimensional disordered hard-point gas [9]. It has been found that ZT diverges as a power-law in thermodynamic limit, $ZT \propto N^b$, where N is the average number of particles in the system and $b \approx 0.79$. Even though the above result could be, in principle, very interesting, no indication was given concerning the microscopic mechanism which is responsible for the increase of ZT . On the other hand a theoretical understanding is needed in order to obtain useful hints for increasing thermodynamic efficiency in more realistic models.

In this paper, we propose a mechanism which explains the large thermoelectric quality factor ZT numerically observed in Ref. [9]. This mechanism requires local equilibrium, as naturally expected in systems with the mixing property, and the emergence, in the linear response regime, of an out-of-equilibrium “modified Maxwell-Boltzmann velocity distribution” of width much larger than the mean velocity of the particle flow. Such broad distribution limit is opposite to the limit of peaked distribution, corresponding to the delta-like energy filtering put forward in Refs. [5, 6]. We provide numerical evidence supporting the effectiveness of the broad-distribution mechanism in

the hard-point gas model.

Our paper is organized as follows. Secs. 2, 3, and 4 review introductory material on coupled particle and energy transport, modeling stochastic baths, and thermoelectric efficiency of the one-dimensional ideal non-interacting gas. In Sec. 5, we present numerical results for thermodynamic transport coefficients for the disordered hard-point gas model. Finally, the obtained numerical results are explained in terms of a mechanism based on the emergence of a broad stationary out-of-equilibrium velocity distribution. Concluding remarks are drawn in Sec. 6.

2. The thermoelectric figure of merit ZT

Let us focus our attention on a conductor in which both electric and heat current flow in one dimension (say, parallel to the x -direction). Assuming local equilibrium, a local entropy (per unit volume) s can be defined, and the rate of entropy production reads [10]

$$\dot{s} = J_u \partial_x \left(\frac{1}{T} \right) + J_\rho \partial_x \left(-\frac{\mu}{T} \right), \quad (1)$$

in which J_u and J_ρ are the energy and particle current densities (fluxes) and $\partial_x(1/T)$, $-\partial_x(\mu/T)$ the associated generalized forces (affinities), where T is the temperature and μ the electrochemical potential.

Assuming that the generalized forces are small, the relationship between fluxes and forces is linear and described by the phenomenological non equilibrium thermodynamic kinetic equations [10, 11]

$$J_u = L_{uu} \partial_x \left(\frac{1}{T} \right) + L_{u\rho} \partial_x \left(-\frac{\mu}{T} \right), \quad (2)$$

$$J_\rho = L_{\rho u} \partial_x \left(\frac{1}{T} \right) + L_{\rho\rho} \partial_x \left(-\frac{\mu}{T} \right), \quad (3)$$

with $L_{\alpha,\beta}$ ($\alpha, \beta \in \{u, \rho\}$) Onsager coefficients. In the absence of magnetic fields, due to microscopic reversibility of the dynamics, the Onsager reciprocity relation $L_{u\rho} = L_{\rho u}$ holds.

In analogy with the relation $dQ = TdS$, the heat current density J_q can be defined by the relation

$$J_q = T J_s, \quad (4)$$

with

$$J_s = \frac{1}{T}J_u - \frac{\mu}{T}J_\rho \quad (5)$$

current density of entropy, and therefore

$$J_q = J_u - \mu J_\rho. \quad (6)$$

The entropy production rate equation can then be written in terms of the fluxes J_q and J_ρ and of the corresponding generalized forces $\partial_x(1/T)$ and $-(1/T)\partial_x\mu$:

$$\dot{s} = J_q \partial_x \left(\frac{1}{T} \right) + J_\rho \left(-\frac{\partial_x \mu}{T} \right), \quad (7)$$

while the linear relationship between fluxes and forces reads as follows:

$$J_q = \tilde{L}_{qq} \partial_x \left(\frac{1}{T} \right) + \tilde{L}_{q\rho} \left(-\frac{\partial_x \mu}{T} \right), \quad (8)$$

$$J_\rho = \tilde{L}_{\rho q} \partial_x \left(\frac{1}{T} \right) + \tilde{L}_{\rho\rho} \left(-\frac{\partial_x \mu}{T} \right), \quad (9)$$

with $\tilde{L}_{\rho\rho} = L_{\rho\rho}$, $\tilde{L}_{q\rho} = \tilde{L}_{\rho q}$ (Onsager relation), $\tilde{L}_{q\rho} = L_{u\rho} - \mu L_{\rho\rho}$, $\tilde{L}_{qq} = L_{uu} - 2\mu L_{u\rho} + \mu^2 L_{\rho\rho}$. Note that, if we call \mathbf{L} and $\tilde{\mathbf{L}}$ the 2×2 Onsager matrices with matrix elements $L_{\alpha\beta}$ ($\alpha, \beta \in \{u, \rho\}$) and $\tilde{L}_{\gamma\delta}$ ($\gamma, \delta \in \{q, \rho\}$), it turns out that $\det \tilde{\mathbf{L}} = \det \mathbf{L}$.

The Onsager coefficients can be expressed in terms of more familiar quantities, the electric conductivity σ , the thermal conductivity κ , and the Seebeck coefficient (thermopower) S . Let us first consider the case in which the thermal gradient vanishes, $\partial_x T = 0$, and the system is homogeneous, so that the chemical potential μ_c is uniform. Since the electrochemical potential μ is composed of a chemical part μ_c and an electric part μ_e , $\mu = \mu_c + \mu_e$, it turns out that for a homogeneous isothermal system $\partial_x \mu = \partial_x \mu_e$. The electric current $J_e = eJ_\rho$, with e charge of the conducting particles, is then given by $J_e = \sigma \mathcal{E} = -(\sigma/e)\partial_x \mu_e$, with \mathcal{E} external electric field applied to the system. The quantities μ_c and μ_e cannot be determined separately by the theory of irreversible thermodynamics [12]: only their combination $\mu = \mu_c + \mu_e$ appears in the kinetic equations (2) and (3). Based on this equivalence, we can write $J_\rho = J_e/e = -(\sigma/e^2)\partial_x \mu$ even when $\mu_c \neq 0$, provided $\partial_x T = 0$, whence Eq. (9) gives

$$\sigma = \frac{e^2}{T} \tilde{L}_{\rho\rho} = \frac{e^2}{T} L_{\rho\rho}. \quad (10)$$

The heat conductivity κ is defined as the heat current density per unit temperature gradient for zero electric current: $J_q = -\kappa\partial_x T$, at $J_e = 0$. Solving the two kinetic equations (8) and (9) simultaneously, we obtain

$$\kappa = \frac{1}{T^2} \frac{\det \tilde{\mathbf{L}}}{\tilde{L}_{\rho\rho}} = \frac{1}{T^2} \frac{\det \mathbf{L}}{L_{\rho\rho}}. \quad (11)$$

Finally, the Seebeck coefficient S is defined as the change in electro-chemical potential per unit charge, $-\partial_x\mu/e$, per unit change in temperature difference: $S = -(1/e)\partial_x\mu/\partial_x T$, at $J_e = 0$. We then obtain from Eq. (9)

$$S = \frac{\tilde{L}_{q\rho}}{eT\tilde{L}_{\rho\rho}} = \frac{1}{eT} \left(\frac{L_{u\rho}}{L_{\rho\rho}} - \mu \right). \quad (12)$$

It is of course possible to eliminate the three Onsager coefficients \tilde{L}_{qq} , $\tilde{L}_{q\rho}$, and $\tilde{L}_{\rho\rho}$ from the kinetic equations (8) and (9), and rewrite such equations in terms of the conductivities σ and κ , and of the thermopower S :

$$J_q = -(\kappa + T\sigma S^2)\partial_x T - \frac{T\sigma S}{e}\partial_x\mu, \quad (13)$$

$$J_\rho = -\frac{\sigma}{e^2}\partial_x\mu - \frac{\sigma S}{e}\partial_x T. \quad (14)$$

By eliminating $\partial_x\mu$ from the above two equations one can express J_q in terms of J_ρ and $\partial_x T$. It is then easy to derive an interesting expression for the entropy current density $J_s = J_q/T$ [10]:

$$J_s = eSJ_\rho - \frac{\kappa}{T}\partial_x T, \quad (15)$$

from which the Seebeck coefficient can be understood as the entropy transported (per unit charge) by the electron flow. The second contribution to the entropy flow, namely the term $-(\kappa/T)\partial_x T$, is independent of the particle current.

The thermoelectric efficiency η , of converting the input heat into output work, is determined by the non-dimensional figure of merit

$$ZT \equiv \frac{\sigma S^2}{\kappa} T. \quad (16)$$

To derive the relation between η and ZT , we consider a one-dimensional system whose left/right ends are connected with left/right thermochemical

reservoirs, with small temperature difference $\Delta T \equiv T_R - T_L$ and electrochemical potential difference $\Delta\mu \equiv \mu_R - \mu_L$. The efficiency η is given, under steady state conditions, by the ratio of the time derivatives of the extracted work over the heat leaving the hot reservoir:

$$\eta = \frac{\dot{W}}{\dot{Q}} = \frac{\Delta\mu J_\rho}{J_q}. \quad (17)$$

Using Eqs. (13) and (14) to eliminate $\partial_x\mu$ and J_q , we obtain

$$\eta = \eta_C \frac{T}{\sigma \partial_x T} \frac{J_e^2 + \sigma S \partial_x T J_e}{T S J_e - k \partial_x T}, \quad (18)$$

where $\eta_C = 1 - T_R/T_L$ is the Carnot efficiency (here we assume $T_L > T_R$). The maximum efficiency for a given ΔT is derived after optimizing (18) with respect to J_e :

$$\eta_{\max} = \eta_C \frac{\sqrt{ZT+1} - 1}{\sqrt{ZT+1} + 1}. \quad (19)$$

The Carnot efficiency is therefore achieved in the limit $ZT \rightarrow \infty$.

Using Eqs. (10), (11), and (12), we can express ZT in terms of the Onsager coefficients:

$$ZT = \frac{\tilde{L}_{q\rho}^2}{\det \tilde{\mathbf{L}}} = \frac{(L_{u\rho} - \mu L_{\rho\rho})^2}{\det \mathbf{L}}. \quad (20)$$

The only thermodynamic restrictions to the Onsager coefficients come from the positivity of the entropy production, $\dot{s} \geq 0$, which is a quadratic form in the generalized forces $\partial_x(1/T)$ and $-\partial_x(\mu/T)$ (see Eqs. (1)-(3)) or $\partial_x(1/T)$ and $-(1/T)\partial_x\mu$ (see Eqs. (7)-(9)). Condition $\dot{s} \geq 0$ implies $L_{uu}, L_{\rho\rho} \geq 0$, $\det \mathbf{L} \geq 0$ in the first case, $\tilde{L}_{qq}, \tilde{L}_{\rho\rho} \geq 0$, $\det \tilde{\mathbf{L}} \geq 0$ in the latter. Thus, the only restriction to the thermoelectric figure of merit is $ZT \geq 0$, so that in principle Carnot efficiency can be achieved.

It is clear from Eq. (20) that ZT diverges iff the Onsager matrix \mathbf{L} (or, equivalently, $\tilde{\mathbf{L}}$) is ill-conditioned, that is, when the condition number $\lambda_1(\mathbf{L})/\lambda_2(\mathbf{L})$ diverges, where $\lambda_1(\mathbf{L})$ and $\lambda_2(\mathbf{L})$ are the largest and the smallest eigenvalue of \mathbf{L} , respectively. The condition number diverges iff the quantity

$$\text{cond}(\mathbf{L}) \equiv \frac{[\text{Tr}(\mathbf{L})]^2}{\det(\mathbf{L})} \quad (21)$$

diverges. In this case the system (2)-(3) (or, equivalently, the system (8)-(9)) becomes singular, and therefore $J_u \propto J_\rho$. In short, the Carnot efficiency is obtained iff the energy and particle currents are proportional.

3. Modeling thermochemical baths

We consider a one-dimensional system whose ends are in contact with left/right baths (reservoirs), which are able to exchange energy and particles with the system, at fixed temperature T_α and electrochemical potential μ_α , where $\alpha = L, R$ denotes the left/right bath.

The thermochemical reservoirs are modeled as infinite one-dimensional ideal gases. Therefore, particle velocities in the reservoirs are described by the Maxwell-Boltzmann distribution,

$$f_\alpha(v) = \sqrt{\frac{m}{2\pi k_B T_\alpha}} \exp\left(-\frac{mv^2}{2k_B T_\alpha}\right), \quad (22)$$

where k_B is the Boltzmann constant and m the mass of the particles. We use a stochastic model of the thermochemical baths [13]: Whenever a particle of the system crosses the boundary which separates the system from the left or right reservoir, it is removed. On the other hand, particles are injected into the system from the boundaries, with rates γ_α . The injection rate γ_α is computed by counting how many particle from reservoir α cross the reservoir-system boundary per unit time. That is to say,

$$\gamma_\alpha = \rho_\alpha \int_0^\infty dv v f_\alpha(v) = \rho_\alpha \sqrt{\frac{k_B T_\alpha}{2\pi m}}, \quad (23)$$

with ρ_α density of the ideal gas in reservoir α . Therefore, particles are injected into the system with velocity distribution

$$P_\alpha(v) = \frac{m}{k_B T_\alpha} v \exp\left(-\frac{mv^2}{2k_B T_\alpha}\right) \theta_\alpha(v), \quad (24)$$

where $\theta_\alpha(v)$ are step functions: $\theta_L(v) = 1$ if $v \geq 0$, 0 otherwise; $\theta_R(v) = 1$ if $v \leq 0$, 0 otherwise. We assume that injections from a macroscopic reservoir are independent events and that the time interval between subsequent injections satisfies the Poissonian distribution,

$$\mathcal{P}_\alpha(t) = \gamma_\alpha \exp(-\gamma_\alpha t), \quad (25)$$

so that the average time between injections is $1/\gamma_\alpha$.

In order to relate the density ρ_α to the electrochemical potential μ_α , it is convenient to write the grand partition function

$$\Xi_\alpha = \sum_{N=0}^{\infty} \frac{1}{N!} \left\{ \frac{\Lambda}{h} e^{\beta_\alpha \mu_\alpha} \int dv m \exp\left[-\beta_\alpha \left(\frac{1}{2}mv^2\right)\right] \right\}^N, \quad (26)$$

with Λ and N size and number of particles of the reservoir, respectively ¹, $\beta_\alpha \equiv 1/(k_B T_\alpha)$ and h the Planck's constant. We then compute the average number of particles as

$$\langle N \rangle_\alpha = \frac{1}{\beta_\alpha} \frac{\partial}{\partial \mu_\alpha} \ln \Xi_\alpha, \quad (27)$$

so that

$$\rho_\alpha = \frac{\langle N \rangle_\alpha}{\Lambda} = \frac{e^{\beta_\alpha \mu_\alpha} \sqrt{2\pi m k_B T_\alpha}}{h}. \quad (28)$$

Therefore, we can express the electrochemical potentials of the bath in terms of the injection rates:

$$\mu_\alpha = k_B T_\alpha \ln(\lambda_{T_\alpha} \rho_\alpha), \quad (29)$$

with

$$\lambda_{T_\alpha} = \frac{h}{\sqrt{2\pi m k_B T_\alpha}} \quad (30)$$

de Broglie thermal wave length. Note that this relation, even though derived from the grand partition function of a classical ideal gas, can only be justified if particles are considered as indistinguishable. The $1/N!$ term in the grand partition function (26) is rooted in the above indistinguishability, of purely quantum mechanical origin [14]. The stochastic thermochemical baths used in our numerical simulations are based on Eqs. (23), (24), (25), and (29). The electrochemical potential μ_α and the temperature T_α can be controlled by varying the injection rate γ_α and the temperature T_α .

4. One-dimensional non-interacting classical gas

Let us first consider the simplest case of a one-dimensional gas of non-interacting particles. Assuming that also the reservoirs are one-dimensional and that the left/right contacts between system and reservoirs are identical and described as in Sec. 3, the particle current J_ρ reads

$$J_\rho = \gamma_L \int_0^\infty d\epsilon u_L(\epsilon) \mathcal{T}(\epsilon) - \gamma_R \int_0^\infty d\epsilon u_R(\epsilon) \mathcal{T}(\epsilon), \quad (31)$$

where $u_\alpha(\epsilon)$ is the energy distribution of the particles injected from reservoir α and $\mathcal{T}(\epsilon)$ is the transmission probability for a particle with energy ϵ to

¹It is of course understood that Λ is macroscopically large and that the thermodynamic limit is eventually taken for the reservoir

transit from one end to the other end of the system, $0 \leq \mathcal{T}(\epsilon) \leq 1$. Using Eq. (24), we obtain

$$u_\alpha(\epsilon) = \beta_\alpha e^{-\beta_\alpha \epsilon}. \quad (32)$$

Furthermore, from Eqs. (23) and (28) we have

$$\gamma_\alpha = \frac{1}{h\beta_\alpha} e^{\beta_\alpha \mu_\alpha}. \quad (33)$$

After substitution of (32) and (33) into (31), we arrive to the following expression for the particle current:

$$J_\rho = \frac{1}{h} \int_0^\infty d\epsilon \left(e^{-\beta_L(\epsilon - \mu_L)} - e^{-\beta_R(\epsilon - \mu_R)} \right) \mathcal{T}(\epsilon). \quad (34)$$

Similarly, we obtain the heat currents $J_{q,\alpha} = J_u - \mu_\alpha J_\rho$ at the left and right reservoirs:

$$J_{q,\alpha} = \frac{1}{h} \int_0^\infty d\epsilon (\epsilon - \mu_\alpha) \left(e^{-\beta_L(\epsilon - \mu_L)} - e^{-\beta_R(\epsilon - \mu_R)} \right) \mathcal{T}(\epsilon). \quad (35)$$

The thermoelectric efficiency is then given by (we assume $T_L > T_R$, $\mu_R > \mu_L$ and consider only $\mathcal{T}(\epsilon)$ functions such that $J_\rho \geq 0$ and $J_{q,L} \geq 0$)

$$\eta = \frac{J_{q,L} - J_{q,R}}{J_{q,L}} = \frac{(\mu_R - \mu_L) \int_0^\infty d\epsilon \left(e^{-\beta_L(\epsilon - \mu_L)} - e^{-\beta_R(\epsilon - \mu_R)} \right) \mathcal{T}(\epsilon)}{\int_0^\infty d\epsilon (\epsilon - \mu_L) \left(e^{-\beta_L(\epsilon - \mu_L)} - e^{-\beta_R(\epsilon - \mu_R)} \right) \mathcal{T}(\epsilon)}. \quad (36)$$

When the transmission is possible only within a tiny energy window around $\epsilon = \epsilon_\star$, the efficiency reads

$$\eta = \frac{\mu_R - \mu_L}{\epsilon_\star - \mu_L}. \quad (37)$$

In the limit $J_\rho \rightarrow 0$, corresponding to reversible transport [6], we get ϵ_\star from Eq. (34):

$$\epsilon_\star = \frac{\beta_L \mu_L - \beta_R \mu_R}{\beta_L - \beta_R}. \quad (38)$$

Substituting such ϵ_\star in Eq. (37), we obtain the Carnot efficiency $\eta = \eta_C = 1 - T_R/T_L$. Such delta-like energy-filtering mechanism for increasing thermoelectric efficiency has been pointed out in Refs. [5, 6].

In the linear response regime, using a delta-like energy filtering, $\mathcal{T}(\epsilon) = 1$ in a tiny interval of width $\delta\epsilon$ around some energy $\bar{\epsilon}$, 0 otherwise, we obtain

$$L_{uu} = \frac{L\bar{\epsilon}^2(\delta\epsilon)}{hk_B} e^{-\beta(\bar{\epsilon} - \mu)}, \quad L_{u\rho} = L_{\rho u} = \frac{L\bar{\epsilon}(\delta\epsilon)}{hk_B} e^{-\beta(\bar{\epsilon} - \mu)}, \quad L_{\rho\rho} = \frac{L(\delta\epsilon)}{hk_B} e^{-\beta(\bar{\epsilon} - \mu)}, \quad (39)$$



Figure 1: Schematic picture of the model considered in our numerical simulations.

where L is the length of system. From these relations we immediately derive that the Onsager matrix is ill-conditioned and therefore $ZT = \infty$ and $\eta = \eta_C$. We point out that the parameters $\bar{\epsilon}$ and $\delta\epsilon$ characterizing the transmission window, appear in the Onsager matrix elements (39) and therefore are assumed to be independent of the applied temperature and electrochemical potential gradients. On the other hand, the energy ϵ_\star in Eqs. (37),(38) depends on the applied gradients. There is of course no contradiction since (37),(38) have general validity beyond the linear response regime.

5. One-dimensional interacting classical gas

Let us now turn to the interacting case. We consider a one-dimensional, di-atomic disordered chain, of hard-point elastic particles with coordinates $x_i \in [0, L]$, L being the system size, velocities v_i and masses $m_i \in \{m, M\}$ randomly distributed. The particles interact among themselves through elastic collisions only. A schematic picture of the model is drawn in Fig. 1. Since we are considering a purely mechanical model, strictly speaking we are going to investigate thermodiffusion rather than thermoelectricity. On the other hand, we assume that the particles are charged and that the Coulomb repulsion is screened and modeled by a short-range hard-core interaction (elastic collisions). Therefore, our model is relevant also for thermoelectricity. Numerical results obtained in Ref. [9] suggest that, for mass ratio $M/m \neq 1$, the figure of merit ZT diverges in the thermodynamic limit.²

Let ℓ be a reference unit length which we take 1 in simulations. In our numerical simulations we set $\mu = (\mu_L + \mu_R)/2 = 0.2[h^2/m\ell^2]$ and $T = (T_L + T_R)/2 = 3.0[h^2/m\ell^2 k_B]$, and consider μ_L, μ_R, T_L, T_R slightly different from the mean values μ, T to drive finite currents J_ρ and J_u . We assume that

²The two masses must be different in order to have ergodic and mixing dynamics, so that thermalization within the system occurs. For equal masses the dynamics is integrable and $ZT = 1$ [9].

the mass of each particle injected by the left or right bath is chosen randomly and with equal a priori probabilities between the two possible values m and M . The average currents J_u and J_ρ are computed at the contacts between system and baths: If, in a period of time t the left bath injects N_i particles with masses $m_j^{(i)}$ and velocities $v_j^{(i)}$, $j = 1, \dots, N_i$, and absorbs N_a particles with masses $m_j^{(a)}$ and velocities $v_j^{(a)}$, $j = 1, \dots, N_a$, then in the large t limit the currents J_ρ and J_u are given by

$$J_\rho = \frac{1}{t}(N_i - N_a), \quad (40)$$

$$J_u = \frac{1}{t} \left(\sum_{j=1}^{N_i} \frac{1}{2} m_j^{(i)} [v_j^{(i)}]^2 - \sum_{j=1}^{N_a} \frac{1}{2} m_j^{(a)} [v_j^{(a)}]^2 \right). \quad (41)$$

Note that in the steady state, due to particle and energy conservation, these currents are equal to the corresponding currents computed for the right bath. Then the Onsager matrix elements from which σ , S , κ , and ZT can be readily derived, are obtained from Eqs. (8) and (9). We set the mass ratio $M/m = \pi$ and calculate currents up to $L = 80[\ell]$, corresponding to an average number of particles inside the system $\langle N \rangle \approx 515$.

In Fig. 2, we present our numerical results for the transport coefficients. A power law dependence for σ/L , κ/L , and ZT is observed³. In particular, the figure of merit ZT increases with increasing the systems size, $ZT \propto L^{0.79}$. Correspondingly, the condition number $[\text{Tr}(\mathbf{L})]^2/\det(\mathbf{L})$ (see Eq. (21)) diverges, as expected from the general theoretical considerations of Sec. 2.

These numerical results naturally raise a question: Is the mechanism leading to high ZT quality factor for interacting gases related to the delta-like mechanism [5, 6] shortly discussed in Sec. 4 for the non-interacting ideal gas? To address this question, we measure the particle current at the position $x \in [0, L]$ as

$$J_\rho = \int_0^\infty dE D(E), \quad (42)$$

$$D(E) \equiv D_L(E) - D_R(E), \quad (43)$$

where the “transmission function” $D_L(E)$ is the density of particles with energy E crossing x and coming from the left side, while $D_R(E)$ is the density

³Numerical data are consistent with those reported in Ref. [9] for the same mass ratio.

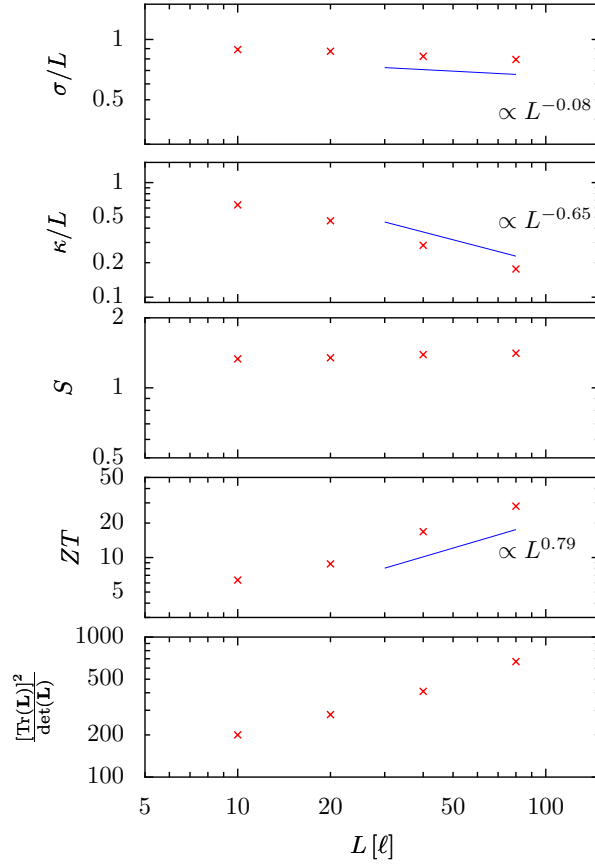


Figure 2: Thermoelectric transport properties. The quantities σ/L , κ/L , ZT , and $\frac{[\text{Tr}(\mathbf{L})]^2}{\det(\mathbf{L})}$ show a power law dependence on the system size L .

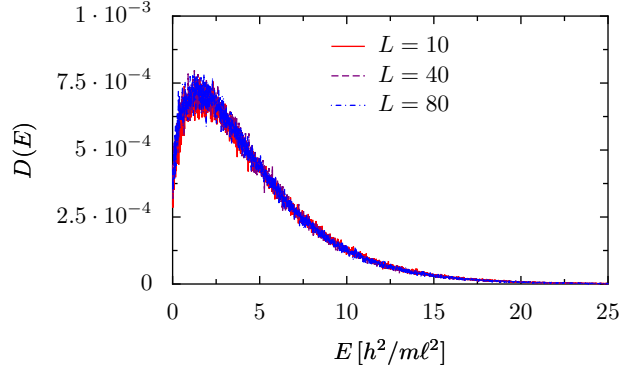


Figure 3: $D(E)$ calculated for $L = 10, 40$ and 80 .

of particles with energy E from the right side. We inquire how $D(E)$ changes as a function of L , in particular if $D(E)$ becomes more and more delta-like (peaked in energy) when increasing L . The transmission function $D(E)$ is shown in Fig. 3, at $x = L/2$ and for different system sizes⁴. There is no sign of narrowing of $D(E)$ when increasing the system size. We can therefore conclude that the mechanism leading to the large ZT values observed in Fig. 2 must be different from the energy filtering discussed in Refs. [5, 6].

To understand the mechanism, we first write the particle and energy currents as

$$J_\rho = \overline{v(x, t) \rho(x, t)}, \quad J_u = \overline{\frac{1}{2} m v(x, t)^3 \rho(x, t)}, \quad (44)$$

where $x \in [0, L]$, the overbar denotes time-averaging, and $v(x, t)$, $\rho(x, t)$ are respectively the particles velocity and density at the position x and time t . If the relaxation time scales for density and velocity are well separated, then expressions (44) can be approximated as:

$$J_\rho \sim \overline{v(x, t)} \times \overline{\rho(x, t)}, \quad J_u \sim \overline{\frac{1}{2} m v(x, t)^3} \times \overline{\rho(x, t)}. \quad (45)$$

In our model, this is satisfied. For instance, in the case of $(\mu_L, \mu_R) =$

⁴Note that, while J_ρ is position-independent due to conservation of particles, $D(E)$ depends on x . However, we have checked that similar behaviors of $D(E)$ are obtained for different values of x .

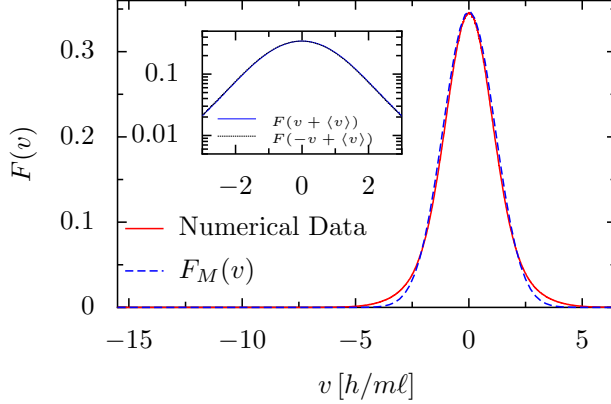


Figure 4: $F(v)$ calculated for the parameters $(\mu_L, \mu_R) = (0.24, 0.16) [h^2/m\ell^2]$, $T = 3.0 [h^2/m\ell^2 k_B]$ with the system size $L = 40$. The solid line corresponds to the numerical data, at $x = L/2$. The mean velocity is $\overline{v(L/2, t)} \sim 0.010 [h/m\ell]$. The dashed line is the modified Maxwell-Boltzmann distribution $F_M(v)$ which fits $F(v)$ with the parameters $\langle v \rangle = \overline{v(L/2, t)} = 0.010 [h/m\ell]$ and $\nu = 1.15 [h/m\ell]$. For these parameters, Eq.(47) yields $\langle v^3 \rangle \sim 0.041$, which is comparable to the exact numerical data $\langle v^3 \rangle \sim 0.047$. The inset shows the behavior of $F(v + \langle v \rangle)$ and $F(-v + \langle v \rangle)$ in the semi-log scale. These two curves completely overlap each other, as expected from Eq. (46). Note that the tails deviate from the Gaussian form.

$(0.24, 0.16) [h^2/m\ell^2]$, $T = 3.0 [h^2/m\ell^2 k_B]$, and $L = 40 [\ell]$, we get at $x = L/2$ the time-averaged velocity $\overline{v(L/2, t)} \approx 0.010 [h/m\ell]$, and the time-averaged density $\overline{\rho(L/2, t)} \approx 6.43 [1/\ell]$, while $\overline{v(L/2, t) \rho(L/2, t)} \approx 0.0641 [h/m\ell^2]$.

From the discussion of Sec. 2, it is clear that ZT diverges when $J_u \propto J_\rho$. According to Eq. (45), this is the case when $\overline{v^3} \propto \overline{v}$. Since we are interested in the steady-state transport properties and we are considering systems with the mixing property, it is natural to assume that the time-averages $\overline{v^n}$ equal the ensemble averages $\langle v^n \rangle \equiv \int_{-\infty}^{+\infty} dv v^n F(v)$, with $F(v)$ velocity distribution function for the steady state. At equilibrium ($T_L = T_R$, $\mu_L = \mu_R$), the system thermalizes and $F(v)$ is the Maxwell-Boltzmann distribution (22) at any x . In the linear response regime, we assume that $F(v)$ is given by a “modified Maxwell-Boltzmann distribution”,

$$F_M(v) = \sqrt{\frac{m^*}{2\pi k_B T}} \exp\left(-\frac{m^*(v - \langle v \rangle)^2}{2k_B T}\right), \quad (46)$$

where the mean velocity $\langle v \rangle$ and the effective mass m^* are fitting parameters,

and $T \approx T_L \approx T_R$. That is to say, we assume that the out-of-equilibrium stationary distribution (46) differs from the equilibrium Maxwell-Boltzmann distribution only in the position $\langle v \rangle$ of the peak, while the Gaussian shape is unchanged. As shown in Fig. 4, such assumption is in good agreement with the numerically computed $F(v)$ close to the peak of the distribution, while the tails show deviations from (46). Nevertheless, such deviations do not affect too much the values of $\langle v \rangle$ and $\langle v^3 \rangle$ and Eq. (46) is very convenient for analytical considerations and to unveil the mechanism at the origin of the large thermoelectric efficiencies observed in the hard-point gas model.

From Eq. (46) we obtain

$$\langle v^3 \rangle = \langle v \rangle^3 + 3\nu^2 \langle v \rangle, \quad (47)$$

where

$$\nu \equiv \sqrt{\frac{k_B T}{m^*}} \quad (48)$$

is the width of distribution (46). We obtain $\langle v^3 \rangle \propto \langle v \rangle$ when $\nu \gg \langle v \rangle$, that is, in the broad-distribution limit. It is clear from Fig. 4 that, for the one-dimensional interacting hard-point gas, indeed $\nu \gg \langle v \rangle$.⁵

6. Conclusions

We have studied numerically the coupled particle and energy transport in a prototype model of interacting one-dimensional gas: the disordered, hard-point gas. There is numerical evidence that the ZT quality factor diverges with increasing the system size. We explain this result in terms of the emergence of a broad velocity distribution of the particles transmitted across the sample. This mechanism first of all requires local equilibrium, which is expected to take place in systems with the mixing property. We also make a couple of assumptions which are quite natural in many-body systems: the separation of the relaxation time scales of density and velocity in Eq. (45), and the modified Maxwell-Boltzmann form of the velocity distribution (46). On the other hand, since $ZT = (\sigma S^2 / \kappa) T$ and Fig. 2 shows that the Seebeck

⁵ Note that the delta-like limit of Eq. (46), $\nu \ll \langle v \rangle$, is incompatible with the linear response regime plus approximation (45) since, if $J_\rho \propto \langle v \rangle$ is a linear function of the applied temperature and electrochemical potential gradients, the same cannot hold for $J_u \propto \langle v^3 \rangle \approx \langle v \rangle^3$.

coefficient is practically constant, the anomalous behavior of σ and κ [15] is crucial to obtain a diverging ZT . The relationship between the broad velocity-distribution mechanism and the anomalous behavior of the transport coefficients must be clarified. In particular, further investigations are required to understand whether this mechanism could be applied to systems with the mixing property but without anomalous transport. It might indeed be possible to find systems in which σ , κ and ZT eventually converge to finite but large values, when increasing the system size. Therefore, our mechanism could be also relevant in more realistic interacting systems with the mixing property.

Acknowledgements

G.B. and G.C. acknowledge support by the MIUR-PRIN 2008 *Efficiency of thermoelectric machines: A microscopic approach*.

- [1] G. Mahan, B. Sales, J. Sharp, Phys. Today 50 (March 1997), 42.
- [2] A. Majumdar, Science 303 (2004) 777.
- [3] M.S. Dresselhaus, G. Chen, M.Y. Tang, R.G. Yang, H. Lee, D.Z. Wang, Z.F. Ren, J.-P. Fleurial, P. Gogna, Adv. Mater. 19 (2007) 1043.
- [4] G.J. Snyder, E.R. Toberer, Nature Materials 7 (2008) 105.
- [5] G.D. Mahan, J.O. Sofo, Proc. Natl. Acad. Sci. USA 93 (1996) 7436.
- [6] T.E. Humphrey, R. Newbury, R.P. Taylor, H. Linke, Phys. Rev. Lett. 89 (2002) 116801; T.E. Humphrey, H. Linke, Phys. Rev. Lett. 94 (2005) 096601.
- [7] M. Terraneo, M. Peyrard, G. Casati, Phys. Rev. Lett. 88 (2002) 094302; B. Li, L. Wang, G. Casati, Phys. Rev. Lett. 93 (2004) 184301; D. Segal, A. Nitzan, Phys. Rev. Lett. 94 (2005) 034301; B. Hu, L. Yang, and Y. Zhang, Phys. Rev. Lett. 97 (2006) 124302; N. Yang, N. Li, L. Wang, B. Li, Phys. Rev. B 76, 020301(R) (2007); B. Li, L. Wang, G. Casati, Appl. Phys. Lett. 88 (2006) 143501; L. Wang and B. Li, Phys. World 21 (2008) 27; N. Li, F. Zhan, P. Hänggi, B. Li, Phys. Rev. E 80 (2009) 011125, and references therein.

- [8] G. Casati, C. Mejía-Monasterio, T. Prosen, Phys. Rev. Lett. 101 (2008) 016601.
- [9] G. Casati, L. Wang, T. Prosen, J. Stat. Mech. (2009) L03004.
- [10] H.B. Callen, Thermodynamics and an Introduction to Thermostatistics (second edition), John Wiley & Sons, New York, 1985.
- [11] S.R. de Groot, P. Mazur, Non-Equilibrium Thermodynamics, Dover, New York, 1984.
- [12] P.L. Walstrom, Am. J. Phys. 56 (1988) 890.
- [13] C. Mejía-Monasterio, H. Larralde, F. Leyvraz, Phys. Rev. Lett. 86 (2001) 5417; H. Larralde, F. Leyvraz, C. Mejía-Monasterio, J. Stat. Phys. 113 (2003) 197.
- [14] K. Huang, Statistical Mechanics (second edition), John Wiley & Sons, New York, 1987, Sec. 6.6.
- [15] S. Lepri, R. Livi, A. Politi, Phys. Rep. 377 (2003) 1.